INSTITUTE OF PHYSICS PUBLISHING CLASSICAL AND QUANTUM GRAVITY

Class. Quantum Grav. **20** (2003) 2917–2928 PII: S0264-9381(03)59947-6

Mechanical loss in tantala/silica dielectric mirror coatings

Steven D Penn[1,6], Peter H Sneddon[2], Helena Armandula[3], Joseph C Betzwieser[4], Gianpietro Cagnoli[2], Jordan Camp[3,7], D R M Crooks[2], Martin M Fejer[5], Andri M Gretarsson[1,8], Gregory M Harry[4], Jim Hough[2], Scott E Kittelberger[1], Michael J Mortonson[4], Roger Route[5], Sheila Rowan[5] and Christophoros C Vassiliou[4]

[1] Department of Physics, Syracuse University, Syracuse, New York 13244-1130, USA
[2] Department of Physics and Astronomy, University of Glasgow, Glasgow G12 8QQ, UK
[3] LIGO Laboratory, California Institute of Technology, Pasadena, CA 91025, USA
[4] LIGO Laboratory, Massachusetts Institute of Technology, Cambridge, MA 02139, USA
[5] Edward L Ginzton Laboratory, Stanford University, Stanford, CA 94305-4085, USA

Received 24 February 2003
Published 12 June 2003
Online at stacks.iop.org/CQG/20/2917

Abstract

Current interferometric gravitational wave detectors use test masses with mirror coatings formed from multiple layers of dielectric materials, most commonly alternating layers of SiO_2 (silica) and Ta_2O_5 (tantala). However, mechanical loss in the Ta_2O_5/SiO_2 coatings may limit the design sensitivity for advanced detectors. We have investigated sources of mechanical loss in the Ta_2O_5/SiO_2 coatings, including loss associated with the coating–substrate interface, with the coating–layer interfaces and with the coating materials. Our results indicate that the loss is associated with the coating materials and that the loss of Ta_2O_5 is substantially larger than that of SiO_2.

PACS numbers: 04.80.Nn, 95.55.Ym, 62.40.+i, 68.35.Gy

(Some figures in this article are in colour only in the electronic version)

1. Introduction

The sensitivity of designs for advanced interferometric gravitational wave detectors, such as Advanced LIGO (Laser Interferometer Gravitational Wave Observatory), is limited in

[6] Present address: Department of Physics, Hobart and William Smith Colleges, Geneva, New York, 14456, USA.
[7] Present address: Laboratory for High Energy Astrophysics, NASA/Goddard Space Flight Center, Greenbelt, Maryland, 20771, USA.
[8] Present address: LIGO Livingston Observatory, Livingston, Louisiana, 70754, USA.

the frequency range from 10s to 100s of Hz by thermal noise from the main test masses and their suspensions [1]. These test masses, which under current design plans will be formed from either fused silica or sapphire, will each be supported using a fused silica suspension, and will have multi-layer, dielectric mirror coatings [2]. In the current generation of gravitational wave detectors, the test mass mirror coatings are formed by ion-sputtering alternating layers of silicon dioxide (SiO_2) and tantalum pentoxide (Ta_2O_5). This type of coating was chosen because it can be made highly reflective in a narrow band around 1.064 μm, the laser wavelength chosen for LIGO, while having very low absorption and scatter losses [3].

For the past several years, many research groups in the gravitational wave field have been concerned that dielectric coatings could be an important source of thermal noise. This concern was strengthened by Levin's calculation [4] which indicated that mechanical losses in the mirror surface of a test mass could be much greater than had been generally appreciated. Subsequently, our investigations of mirror coatings showed that multi-layers of Ta_2O_5/SiO_2 and Ta_2O_5/Al_2O_3 when applied to fused silica substrates, add significant levels of mechanical loss [5, 6]. Using these results and models developed by Nakagawa [7], and Gretarsson [6], we calculated that mechanical loss in the coatings would result in a level of thermal noise which would degrade the design sensitivity of the planned advanced detectors by a significant amount.

In the present study, we have performed a series of experiments to investigate the source of the loss in multi-layer tantala/silica coatings. We hypothesized that the loss would arise primarily either from the coating–substrate interface, from the coating–layer interfaces, from the coating materials or possibly from some combination of these sources. We have measured the loss of a series of coatings in which the number and thickness of the coating layers was chosen to test each of these dependencies.

2. Design of coating loss study

2.1. Experimental technique

As in our previous experiments [5, 6], we determine the level of mechanical loss associated with a given coating by applying the coating to fused silica substrates and measuring the mechanical losses of a subset of resonant modes of the coated samples.

The mechanical loss, ϕ, at a resonant frequency, f_0, of a sample is related to the quality factor, Q, at the resonance by $\phi(f_0) = 1/Q$. Assuming all other losses to be negligible, the total loss in a coated sample, $\phi_{\text{total}}(f_0)$, is equal to the sum of the intrinsic loss of the substrate plus any loss associated with the coating [5, 6],

$$\phi_{\text{total}}(f_0) \approx \phi_{\text{s}}(f_0) + \frac{E_{\text{c}}}{E_{\text{s}}}\phi_{\text{c}}(f_0) \tag{1}$$

where the subscripts 'c' and 's' denote coating and substrate, respectively, and $E_{\text{c}}/E_{\text{s}}$ is the ratio of energy stored in the coating to energy stored in the substrate. The term, ϕ_{c}, includes the losses in the coating materials, in the coating interfaces and in the coating–substrate interface, all of which are scaled by the energy ratio, $E_{\text{c}}/E_{\text{s}}$. Specifically

$$\phi_{\text{c}} = \phi_{\text{cm}} + \frac{s_{\text{ci}}}{s_{\text{c}}}\phi_{\text{ci}} + \frac{s_{\text{csi}}}{s_{\text{c}}}\phi_{\text{csi}} \qquad (s_{\text{csi}}, s_{\text{ci}} \ll s_{\text{c}})$$

where s is the thickness, and the subscripts 'cm', 'ci' and 'csi' refer to coating materials, coating interfaces and coating–substrate interface, respectively.

In this study, the substrates were 7.6 cm diameter fused silica discs of two different thicknesses, 2.5 cm and 0.25 cm. The thinner discs had the advantage that the effect from

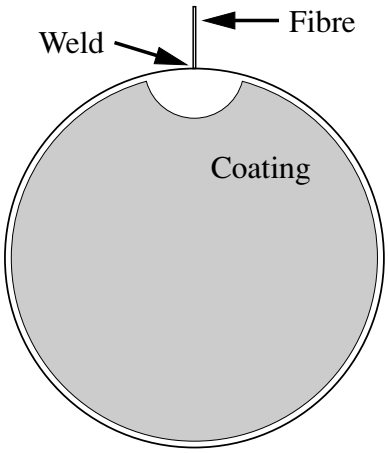

Figure 1. Coating on thin sample with semicircular mask around weld.

the coating was more pronounced; the coating loss had a greater contribution to the total loss because the energy ratio, E_c/E_s, was larger for the thin samples. However, suspending these thin samples required the direct welding of a low-loss silica suspension to the edge of the fused silica substrates; see [6]. To minimize any potential damage to the coatings by direct heat from welding, the coating was masked in a 1 cm radius around the weld; see figure 1. In addition, we used miniature welding torches that allowed the weld area to be sub-millimetre in scale. During welding, the glass $\approx$1 cm from the weld remained only warm to the touch, which suggests that there was little to no impact on the coating. Although measurements of the loss factors of the thicker samples were less sensitive to the effects of coating losses, they had the advantage that they could be suspended using thin silk thread (see [5]) without any risk of physically altering the substrate or the coating.

The use of both techniques allowed a more thorough investigation of mechanical losses in the coating over a wider range of frequencies [8].

The substrates were made of Corning 7980 grade 0A fused silica[9]. Their faces were polished to sub-angstrom micro-roughness by WavePrecision Inc.[10], to emulate the required surface properties of actual test masses. Except where otherwise noted, all the coatings were applied by SMA/Virgo[11] at *l'Institut de Physique Nucleaire* in Lyon France.

To measure the quality factor of a given mode of a sample, we suspended the sample in vacuum and excited it to resonance using an electrostatic drive. We then removed the excitation signal and recorded the sample's motion as it freely rang down. The characteristic decay time, τ, was the time required for the amplitude of motion to decrease by a factor $1/e$. The quality factor was then given by $Q = \pi f_0 \tau$. The amplitude of the resonant motion was sensed interferometrically for the thick (2.5 cm) samples, and by polarimetry for the thin (0.25 cm) samples. At the vacuum pressure for the experiment, ($P \leqslant 10^{-6}$ torr), air damping was negligible. Detailed descriptions of these ringdown techniques are given in [5] and [6], respectively.

We performed finite-element analysis, with the program ALGOR[12], to model the displacement of each mode of the samples. The relevant energy ratios for the coated samples

[9] Corning Incorporated, Corning, New York 14831-0001, USA.
[10] WavePrecision Inc., 5390 Kazuko Court, Moorpark, CA 93021, USA.
[11] *Service des Materiaux Avances/Virgo*, Lyon, France.
[12] ALGOR, Inc, 150 Beta Drive, Pittsburgh, PA 15238-2932, USA.

Table 1. Set of samples used to probe the source of the mechanical loss in the Ta_2O_5/SiO_2 coating.

Sample type	Total layers	Optical thickness		Comments
		SiO_2	Ta_2O_5	
A	0	0	0	Annealed only
B	2	$\lambda/4$	$\lambda/4$	Coated and annealed
C	30	$\lambda/4$	$\lambda/4$	Coated and annealed
D	60	$\lambda/8$	$\lambda/8$	Coated and annealed
E	30	$\lambda/8$	$3\lambda/8$	Coated and annealed
F	30	$3\lambda/8$	$\lambda/8$	Coated and annealed

were then calculated from the displacements [5]. If the intrinsic mechanical loss of the substrate, $\phi_s(f_0)$, is known (or is insignificant compared to the effective loss from the applied coating), the loss associated with the coating may then be calculated using equation (1).

2.2. Sequence of coatings studied

We investigated three primary sources of mechanical loss in the coatings, which we postulated to be

- loss in the coating–substrate interface,
- loss in the interfaces between the multiple coating layers, and
- loss in the coating materials.

To investigate these hypotheses, we designed a set of coatings in which we varied the number and thickness of the coating layers to test for the three dependencies. Table 1 lists the coatings and the substrate treatments investigated. By comparing the measured mechanical loss for sample types B through F, we can test our three hypotheses for the source of the coating loss.

If the dominant source of coating mechanical loss is associated with the coating–substrate interface, then the total loss measured for sample types B-F would be expected to be approximately equal.

On the other hand, the loss may have originated predominantly in the interfaces between the multiple coating layers. In that case the coating loss of sample type D, which has 60 layers, should be twice as large as the loss in sample types C, E and F, which have 30 layers.

Finally, the source of dissipation may be intrinsic to the coating material. Under that scenario, the coating loss for sample types C, E and F should vary with the abundances of the two coating materials.

Clearly there also exists the possibility that the total mechanical loss of the coating is the sum of contributions from a combination of the above mechanisms.

As part of the coating process, samples are heated to a few hundred degrees to reduce residual stresses in the coating. Previous experiments [9–11] have shown that heating uncoated fused silica samples can result in a significant decrease in loss. Coating type A was not coated but was cleaned and heated to the same elevated temperature as the coated samples to ensure any change in substrate loss was taken into account in our analysis. We will refer to this process as 'annealing' even though the samples were not raised to the standard annealing temperatures for fused silica.

Table 2. Results for thin sample measurements. All Qs are $\times 10^6$. All ϕs are $\times 10^{-4}$.

Sample		Butterfly × mode			Butterfly + mode			Drumhead mode			Coating thickness	
Type	Number	Q_{initial}	Q_{total}	ϕ_{coating}	Q_{initial}	Q_{total}	ϕ_{coating}	Q_{initial}	Q_{total}	ϕ_{coating}	s_{silica} (μm)	s_{tantala} (μm)
A	1	14.7		N/A	11.7	43.6	N/A				Uncoated, annealed at 600 °C	
A	2	10.6	42.4	N/A	13.9	54.0	N/A				Uncoated, annealed at 900 °C	
B	1	24.2	9.0	2.4	25.2	8.0	2.7				0.183	0.131
B	2	6.32	5.4	4.0	7.53	6.5	3.3	6.4	3.2		0.183	0.131
C	1	18.4	0.53	2.7	20.8	0.55	2.6				2.75	1.97
C	2	23.1	0.53	2.7	18.6	0.54	2.6	0.43	3.1		2.75	1.97
D	1	17.3	0.49	2.9	20.4	0.55	2.6	0.44	3.1		2.75	1.97
D	2		0.54	2.6	43.6	0.51	2.8				2.75	1.97
E	1	42.4	0.40	3.9	54.0	0.40	3.9	0.29	5.1		1.38	2.95
E	2	22.2	0.40	3.9	20.3	0.41	3.8				1.38	2.95
F	1		0.75	1.8		0.72	1.8				4.13	0.983
F	2		1.13	1.2		0.82	1.6	0.63	2.0		4.13	0.983

3. Results

3.1. Thin sample results

We present below the results of our measurements on the thin samples. We acquired at least five measurements for each mode of a given sample configuration. As is common in Q experiments, we quote the result of the highest measurement. The reason for this selection process is that systematic errors, which in many experiments can equally increase or decrease one's measurement, will, with rare exception in our measurements, uniformly degrade the Q. On the other hand, the statistical errors contribute a uniform, Gaussian background that introduces an error to the fit of Q. Data that does not exhibit uniform background noise are discarded. These statistical errors are normally much smaller that the systematic fluctuations. Therefore, we quote the largest value for our Q measurements with its associated statistical error.

The suspension system, excitation system and data analysis routines have all been tested to produce no limiting effect on measurements where the Q exceeds 80 million. During these measurements, the dimensions of the suspension system and the position of the excitation system were altered with no observed change in the Q of the sample. Finally these measurements were performed at MIT and at Syracuse University with excellent agreement between the two facilities.

The results are listed by mode in table 2. The labels 'initial' and 'total' refer to measurements made before and after the coating and/or annealing process. The mode shapes are shown in figure 2. The butterfly-× and butterfly-+ modes are the degenerate first mode with a typical resonant frequency of $f_1 = 2.7$ kHz. The additional notation of '×' and '+' refers to the orientation of the nodal lines. The second mode, known as the drumhead mode, has a typical resonant frequency of $f_2 = 4.1$ kHz.

One immediate observation from the data is that for the coated samples, with the exception of the 2-layer coating, $Q_{\text{total}} \ll Q_{\text{initial}}$. Typical values for Q_{initial} indicate that the loss in the substrate is about 2–3% of Q_{total} and should not significantly affect the results for the coating loss. Moreover, we see that the annealing performed at the end of the coating run dramatically increases the Q of an uncoated substrate. If we assume that the substrate in a coated sample also experiences the same increase in Q, then the loss in the substrate is reduced to about 1%

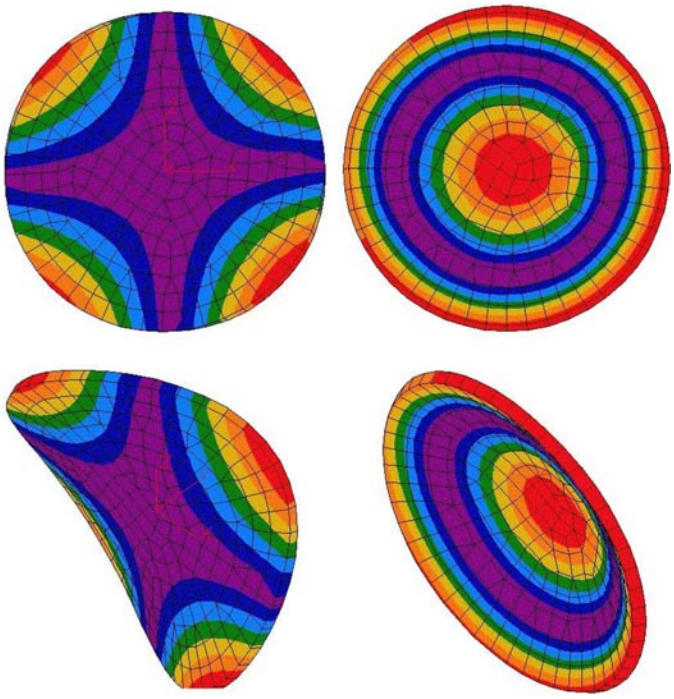

Figure 2. Modes of the thin sample. The first mode (butterfly) on the left and the second mode (drumhead) on the right. The first row is face view and the second row is side view.

of the loss in the coated sample. Thus, for the thin samples, we assume the loss measured in a coated sample is approximately the loss associated with the coating.

$$\phi_{\text{total}} \approx \frac{E_{\text{c}}}{E_{\text{s}}}\phi_{\text{c}}. \tag{2}$$

To calculate the coating losses we require the fraction of the mode energy stored in the coating. This value is calculated from the displacement values obtained using finite-element analysis package, ALGOR (see footnote 12). This analysis yielded an energy ratio per coating thickness of

$$\frac{\mathrm{d}E/\mathrm{d}s}{E} = 1488\ \mathrm{m}^{-1} \quad \text{butterfly mode}$$
$$\frac{\mathrm{d}E/\mathrm{d}s}{E} = 1575\ \mathrm{m}^{-1} \quad \text{drumhead mode.}$$

Then, given the coating thickness, s, we can rewrite the equation for ϕ_{c} as

$$\phi_{\text{total}}(f_0) = s\frac{\mathrm{d}E/\mathrm{d}s}{E}\phi_{\text{c}}(f_0). \tag{3}$$

The coatings are made such that the first layer applied to the substrate is a tantala layer. We convert a coating's optical thickness to its physical thickness using the refractive indices $n_{\text{silica}} = 1.45$ and $n_{\text{tantala}} = 2.03$.

Reviewing our results, listed in table 2, we can test our hypotheses on the source of the coating loss. The first hypothesis was that the coating loss originated in the coating–substrate interface, in which case the loss would be independent of coating thickness. Were this idea true, then coating types B and C, which have 2 and 30 layers, respectively, would have similar

values for Q_{total}. Instead, Q_{total} for these samples differ by a factor 10, and the coating loss, ϕ_{c}, which is scaled for coating thickness, is roughly equal for the two coating types. Thus the loss is in the coating, not the coating–substrate interface ($\phi_{\text{i}} \approx 0$).

Our second idea was that the coating loss arose in the interfaces between the multiple coating layers. To test this hypothesis we can compare the loss for coating types C and D, which have the same total thickness but 30 and 60 layers, respectively. If the loss were dependent on the number of coating interfaces then ϕ_{c} for coating types C and D would differ by a factor 2. However, coating types C and D have similar values for ϕ_{c}, indicating that the loss does not depend on the number of coating interfaces.

Finally if the loss originates in the coating material, then we would expect to see a dependence in ϕ_{c} as the proportions of coating materials are varied in coating types E, C and F. Indeed ϕ_{c} does increase with increasing proportions of Ta_2O_5, indicating that the loss is due to the coating materials.

To separate ϕ_{c} into the losses for the two coating materials, we must partition the energy in the coating into the amounts stored in its silica and tantala layers. Following an analysis by Landau and Lifshitz [12], it can be shown that, for Poisson's ratio, $\sigma \ll 1$, the energy stored in a coating, $E_{\text{c}} \propto Ys$, where Y is Young's modulus and s is the coating thickness. For a multi-layer coating made up of two materials, we may write

$$\phi_{\text{c}} = \frac{Y_1 s_1}{Y_{\text{c}} s_{\text{c}}}\phi_1 + \frac{Y_2 s_2}{Y_{\text{c}} s_{\text{c}}}\phi_2 \tag{4}$$

where Y_i, s_i and ϕ_i are the Young's modulus, total thickness and loss angle of the ith coating material. We use the Young's moduli of 7.2×10^{10} Pa for fused silica and 1.4×10^{11} Pa for tantalum pentoxide [13].

For a thin surface layer, the stress will be predominantly parallel to the surface. In this limit, the total Young's modulus for the multi-layer coating is given by

$$s_{\text{c}} Y_{\text{c}} = s_1 Y_1 + s_2 Y_2. \tag{5}$$

Using equation (5) we rewrite equation (4) as

$$\phi_{\text{c}} = \frac{s_1 Y_1 \phi_1 + s_2 Y_2 \phi_2}{s_1 Y_1 + s_2 Y_2}. \tag{6}$$

Fitting the results for ϕ_{coating} from coating types C, E and F, we obtain the coating material loss values for silica and tantala

$$\begin{aligned}
&\phi_{\text{silica}} = (0.1 \pm 0.1) \times 10^{-4} && \text{(butterfly mode)}\\
&\phi_{\text{tantala}} = (4.7 \pm 0.1) \times 10^{-4} && \text{(butterfly mode)}\\
&\phi_{\text{silica}} = (-0.1 \pm 0.3) \times 10^{-4} && \text{(drumhead mode)}\\
&\phi_{\text{tantala}} = (6.1 \pm 0.3) \times 10^{-4} && \text{(drumhead mode).}
\end{aligned}$$

Note that the losses calculated above are losses for amorphous materials as deposited by an ion beam. The structure of a material in a coating may differ from its typical solid state. Therefore, the measured loss values may be different for the same materials in different states.

As a final consistency check, we measured two samples with coating type C that were coated by MLD[13]. These measurements yielded $\phi_{\text{c}} = 3.0 \times 10^{-4}$ for the butterfly mode, and $\phi_{\text{c}} = 3.2 \times 10^{-4}$ for the drumhead and 2nd butterfly modes. These results are in basic agreement with the samples coated at SMA/Virgo (see footnote 11) and indicate that the coating loss is associated with the materials and not the coating process or manufacturer.

[13] MLD Technologies, 2672 Bayshore Parkway, Suite no 701, Mountain View, CA 94043, USA.

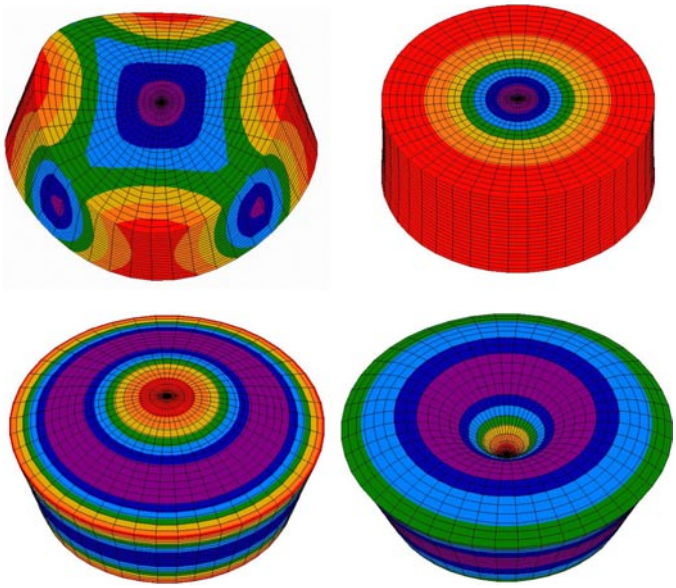

Figure 3. The shapes of the four modes of the thick sample: Clover-4 or butterfly (C4) in upper left; fundamental radial (F) in upper right; asymmetric drumhead (A) in lower left and 2nd asymmetric (2A) in lower right.

3.2. Thick sample results

3.2.1. Initial observations. For the thick fused silica samples (7.6 cm Ø × 2.5 cm thick), we measured the Q factors of four modes both before and after each sample was coated or annealed. The results of these measurements are shown in figure 4. The mode shapes, which were calculated using a finite-element package (see footnote 12), are shown in figure 3.

We suspended the thick samples in a loop of silk thread. Each sample was suspended multiple times, with the suspension length varied each time, and the highest Q factor for each mode was used in our analysis. Previous experiments [14–16] have shown that measured Q factors may be too low if the resonant frequency of a test mass happens to coincide with a resonant frequency of the suspension wires. Using this technique we have shown that suspension losses can be reduced to a negligible level when measuring Qs of the order of a few times 10^7 [5].

Before discussing the quantitative analysis of the results, it is instructive to observe the trends in the data shown in figure 4. Firstly, it can be seen that the Q factors for sample A, which was annealed, and for sample B, which had a 2-layer coating, were very similar, and that these Q factors were considerably higher than the other samples which had thicker coatings. This difference indicates that the coating–substrate interface is not the dominant source of mechanical loss.

Secondly, samples C and D, which have the same total coating thickness, but 30 and 60 coating layers, respectively, have very similar Q factors. This result suggests that the individual multi-layer interfaces are not the dominant source of mechanical loss.

Finally, the coatings on samples C, E and F each have 30 layers and the same total thickness, but vary the proportions of SiO_2 and Ta_2O_5. The measured Qs show that the loss increases with increasing proportions of Ta_2O_5 in the coating. These results suggest that the

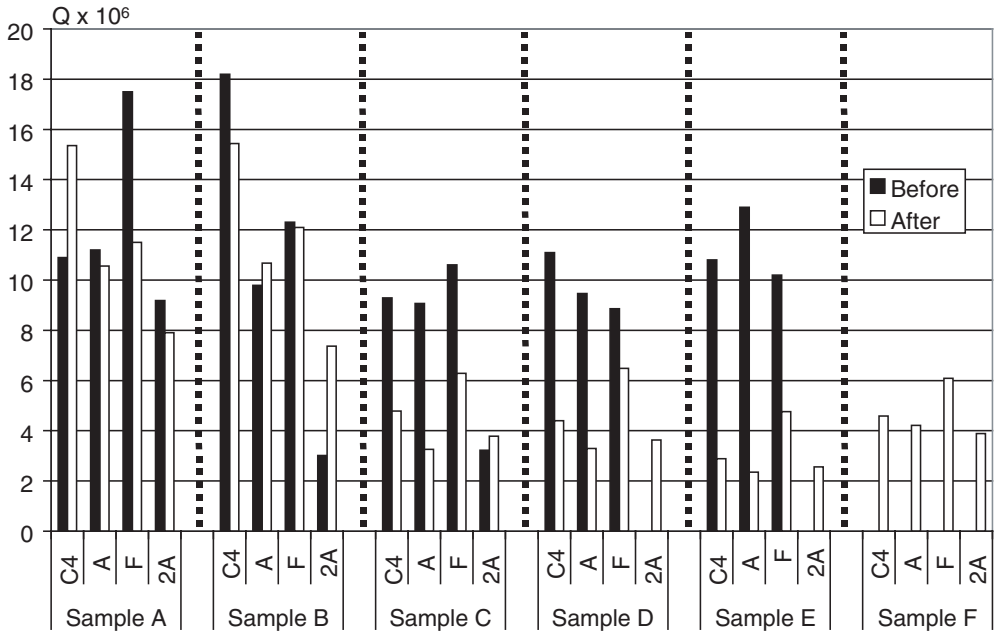

Figure 4. The measured Q values for the four modes of each of the five thick samples with the coatings listed in table 1. The colour of the bar indicates whether the data were measured before (black) or after (white) the coating/annealing process.

coating materials are the dominant source of mechanical loss in the coatings, and that tantalum pentoxide has a higher mechanical loss than silica.

These observations are all consistent with the trends seen in the thinner samples discussed in section 3.1.

It is important to note that the measured Q factors for the samples are mode-dependent. This dependence will be discussed in the following section.

3.2.2. Quantitative analysis. Calculating the coating loss for the thicker samples requires a slightly different method than for the thin samples. For the thin samples, the loss in the substrate was negligible, so the coating loss could be calculated directly from the measured loss in the coated sample. For the thick samples, a much smaller fraction of the energy was stored in the coating. Thus the loss in the substrate must be considered when calculating the loss in the coating.

For each mode of a thick-coated sample, we calculate the energy ratio E_c/E_s. We then rewrite equation (1) as

$$\Delta\phi = \phi_{\text{total}} - \phi_s \approx \frac{E_c}{E_s}\phi_c. \tag{7}$$

To obtain ϕ_c, we plot $\Delta\phi$ versus E_c/E_s for each mode. Figure 5 shows this plot for one sample with 30 alternating layers of SiO_2 and Ta_2O_5. It can be seen that the data appear far from the expected straight line.

From figure 4 it can be seen that there were significant changes in the Q factors of modes of a sample which was annealed but not coated. The Qs of some modes increased while others decreased. In our case, the mechanism for changes in Q is not known but we postulate it may

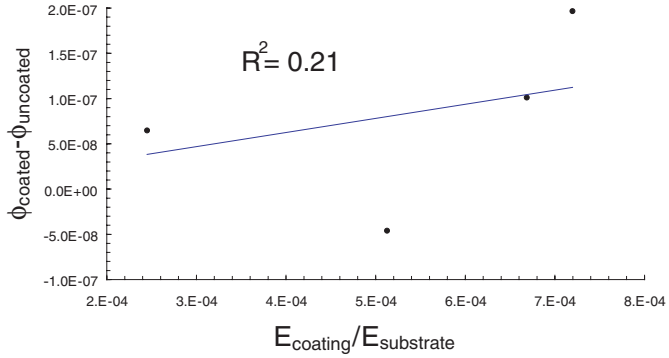

Figure 5. $\Delta\phi(f_0)$ plotted as a function of energy ratio for a typical sample.

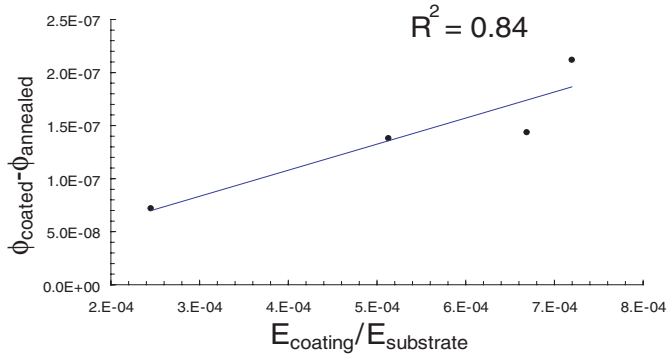

Figure 6. Same sample as in figure 5 except that $\Delta\phi(f_0)$ is corrected to account for the change in substrate loss due to annealing.

be due to some redistribution of stress in the samples, which may produce mode-dependent losses [9]. Thus, while using the measured values for the Q of the uncoated substrate seems invalid, replacing these values by the Q factors of the modes of the annealed, but uncoated mass, should in principle now allow us to obtain a value for $\phi_c(f_0)$. The results of this are shown in figure 6.

It can be seen that there is a significant improvement of the fit to the data using this analysis. Carrying out the same types of analyses on the data from the other coated samples gave very similar results.

3.2.3. Results. The loss factors obtained for each type of coating studied are shown in table 3.

The results shown in table 3 confirm our earlier observations indicating that the dominant source of mechanical loss is associated with the coating materials, and also confirm that the tantalum pentoxide component of the coatings has a higher mechanical loss factor than the silica component. This last deduction can be treated more quantitatively.

As with the thin samples, we use equation (6) and the results for ϕ_c from coating types C, E and F, to calculate the loss for the silica and tantala layers. The results are

$$\phi_{\text{silica}} = (0.5 \pm 0.3) \times 10^{-4} \qquad \phi_{\text{tantala}} = (4.4 \pm 0.2) \times 10^{-4}.$$

Table 3. Mechanical loss factors for the various coating types calculated from the thick sample data.

Coating type	Number of samples	ϕ_{coating}
B	1	$(0.9 \pm 2.8) \times 10^{-4}$
C	2	$(2.7 \pm 0.7) \times 10^{-4}$
D	2	$(2.7 \pm 0.5) \times 10^{-4}$
E	2	$(3.7 \pm 0.5) \times 10^{-4}$
F	2	$(1.9 \pm 0.2) \times 10^{-4}$

We also performed a consistency check on the thick samples by measuring two samples that had coatings of type C applied by MLD (see footnote 13). The measured coating losses were $\phi_c = 2.8 \times 10^{-4}$ for sample 1, and $\phi_c = 3.8 \times 10^{-4}$ for sample 2. Like the thin samples, the thick samples yielded similar results for the two coating manufacturers. In both cases the coatings from MLD (see footnote 13) showed slightly higher loss than the equivalent coatings produced by SMA/Virgo (see footnote 11).

4. Conclusions

For advanced interferometric gravitational wave observatories to be able to reach realistic astronomical distances, low mechanical loss mirror coatings are necessary. Observatories currently in operation use a multi-layer dielectric coating of silica and tantala. We have measured the loss in this coating to be $\phi = 2.7 \times 10^{-4}$, which is in basic agreement with the results from our previous work [5, 6]. Those references discuss how this coating loss may affect the sensitivity of Advanced LIGO. We have shown in this work that the loss in this coating is predominantly the coating material loss in the tantala layers. Work is underway to investigate other coating materials and processes that may give lower mechanical loss while retaining the high reflectivity, low scatter and low optical loss required by these advanced detectors.

Acknowledgments

The US authors would like to thank the National Science Foundation for their support of this work through grants PHY-0140335 (Syracuse), PHY-0140297 (Stanford) and PHY-0107417 (LIGO Laboratory). The UK authors would like to thank PPARC and the University of Glasgow for their financial support.

Addendum

The coating applied to the thick disc as reported in [6] is incorrect. The correct coating thickness of 4.66 μm results in a calculated coating ϕ of 5.2×10^{-4}.

References

[1] Fritschel P (ed) (LIGO Science Collaboration) 2001 *Advanced LIGO System Design*, LIGO-T010075-00-D webpage http://www.ligo.caltech.edu/docs/T/T010075-00.pdf

[2] LIGO Science Collaboration 1999 *LSC White Paper on Detector Research and Development* webpage http://www.ligo.caltech.edu/docs/T/T990080-00.pdf
[3] Srinivasan K, Coyne D and Vogt R 1997 LIGO document LIGO-T97016-00-D webpage http://www.ligo.caltech.edu/docs/T/T970176-00.pdf
[4] Levin Yu 1998 *Phys. Rev.* D **57** 659
[5] Crooks D, Sneddon P, Cagnoli G, Hough J, Rowan S, Fejer M M, Gustafson E, Route R, Nakagawa N, Coyne D, Harry G M and Gretarsson A M 2002 *Class. Quantum Grav.* **19** 883–96
[6] Harry G M, Gretarsson A M, Saulson P R, Penn S D, Startin W J, Kittelberger S E, Crooks D R M, Hough J, Cagnoli G, Nakagawa N, Rowan S and Fejer M M 2002 *Class. Quantum Grav.* **19** 897–918
[7] Nakagawa N, Gretarsson A M, Gustafson E K and Fejer M M 2002 *Phys. Rev.* D **65** 102001
[8] Sneddon P and Rowan S Private communication in preparation
[9] Numata K *et al* 2000 *Phys. Lett.* A **276** 37
[10] Lunin B S and Torbin S N 2000 *Vestnik Moskovskogo Universiteta*, ser 2, *Khimia* **41** 93
[11] Penn S D, Harry G M, Gretarsson A M, Kittelberger S E, Saulson P R, Schiller J J, Smith J R and Swords S O 2001 *Rev. Sci. Instrum.* **72** 3670
[12] Landau L D and Lifshitz E M 1986 *Theory of Elasticity* 3rd edn (Oxford: Pergamon)
[13] Martin P J and Bendavid A *et al* 1993 Mechanical and optical properties of thin films of tantalum oxide deposited by ion-assisted deposition *Thin Films: Stresses and Mechanical Properties IV, Mater. Res. Soc. Symp. Proc.* **308** 583
[14] Braginksy V B, Mitrofanov V P and Panov V I 1985 *Systems with Small Dissipation* (Chicago, II: The University of Chicago Press)
[15] Logan J E, Robertson N A and Hough J 1992 *Phys. Lett.* A **170** 352–8
[16] Rowan S, Twyford S M, Hough J, Gwo D H and Route R 1998 *Phys. Lett.* A **246** 471–8